Available online at www.sciencedirect.com
SCIENCE DIRECT
Polymer 46 (2005) 9033–9042
polymer
www.elsevier.com/locate/polymer

Determining persistence length by size-exclusion chromatography

Thomas Mourey*, Kim Le, Trevor Bryan, Shiying Zheng, Grace Bennett

Research and Development Laboratories, Eastman Kodak Company, 1669 Lake Avenue, Rochester, NY 14615-2136, USA

Received 12 May 2005; received in revised form 29 June 2005; accepted 7 July 2005
Available online 9 August 2005

Abstract

Several methods for determining persistence length from size-exclusion chromatography data are evaluated for a stiff polymer, poly(*n*-hexyl isocyanate) (PHIC), and the more flexible poly[2,7-(9,9 di-*n*-hexylfluorene)]. The molar mass dependence of the root-mean-square radius obtained from light scattering detection is used to calculate the persistence length of PHIC, based on the Kratky–Porod wormlike chain model. The persistence length estimate is in reasonable agreement with literature values, and the results are relatively insensitive to the sample concentration. Directly solving for persistence length by non-linear regression is more suitable than linear approximations that use ratios of root-mean-square radius and molar mass. The persistence length calculated for the same polymer from viscometry detection, and the Yamakawa–Fujii–Yoshizaki hydrodynamic cylinder model for wormlike chains, is reasonable only when the viscosities measured by viscometry detection, and the molar masses measured by light scattering detection, are extrapolated to zero concentration values. The concentration effects are not significant for the more flexible PHF, and viscometry data are suitable for determining persistence lengths, even by linear approximation methods that use the ratio of intrinsic viscosity and molar mass. Molar masses calculated from a universal calibration curve and the viscometry detector are shown to be erroneous for the freely draining PHIC and should not be used for persistence length determination. Other methods that examine selected regions of viscosity conformation plots are shown to be of limited utility.

Keywords: Size-exclusion chromatography; Persistence length; Wormlike chain

1. Introduction

The wormlike or Kratky–Porod (KP) chain model is frequently adopted for stiff and semiflexible macromolecules. It is a special case of the freely rotating chain model for small values of bond angle θ that describe flexibility by fluctuations or bending of a continuous three-dimensional chain contour. Stiffness is reflected in the persistence length, l_p, the distance over which the spatial orientations of monomers are not mutually independent, i.e. the orientation of monomer segments 'persist' from one monomer to the next. The persistent length contains a number of monomer segments of length l, and has length $l_p \sim l2/\theta^2$, and a corresponding Kuhn statistical element of an equivalent freely jointed chain $b \sim 2l_p$. The persistence length can be estimated from the relationship between molar mass, M, and root-mean-square radius, R_g. The relationship changes continuously from rod-like macromolecules with $R_g \propto M$ to $R_g \propto M^{1/2}$ for Gaussian coils, without excluded volume, as M changes from 0 to ∞. Both M and R_g are readily measured by size-exclusion chromatography (SEC) with light scattering detection. Provided the molar mass distribution is broad enough, the transition from rod-like shape to Gaussian coil may be observed in R_g–M conformation plots, and the persistence length can be estimated from a suitable continuous-chain model. In theory, this can be accomplished from the SEC chromatogram of a single sample. Viscosity measured by SEC-viscometry detection and M measured by light scattering detection provides the analogous $[\eta]$–M conformation plot. The Mark–Houwink–Sakuruda viscosity scaling exponent a for intrinsic viscosity $[\eta]$ and M varies according to hydrodynamic theory based on wormlike chains from 1.7 for rods at low values of M to 0.5 for Gaussian coils at large M, without excluded volume. Both R_g and $[\eta]$ conformation plots are distinguished from those of flexible polymers; the slope of plots for wormlike chains is steep at low M and asymptotically approaches a value of 1/2 at large M (no excluded volume), whereas flexible polymers begin with

* Corresponding author. Tel.: +1 585 477 5721; fax: +1 585 477 7781.
E-mail address: thomas.mourey@kodak.com (T. Mourey).

0032-3861/$ - see front matter © 2005 Elsevier Ltd. All rights reserved.
doi:10.1016/j.polymer.2005.07.022

slopes near 1/2 at small M (no excluded volume) and increase in slope with increasing M to values of $\sim$0.59 for the root-mean-square radius and $\sim$0.7–0.8 for intrinsic viscosity as excluded volume effects become significant. The chain stiffness parameters l_p can be estimated from the conformation plots and continuous chain models from the molar mass dependences of R_g and $[\eta]$. This was traditionally performed on narrow molar-mass distribution samples often obtained by solvent fractionation. The temptation to use SEC is considerable. SEC with light scattering and viscometry detection measures molar mass, root-mean-square radius, and intrinsic viscosity on a broad molar mass distribution sample, circumventing the preparation of narrow fractions and potentially improving the accuracy and precision of the results. The measurements are made in dilute solution at concentrations normally below the critical overlap concentration, and the onset of excluded volume effects can usually be observed in conformation plots obtained from SEC with light scattering and viscometry detection. The experiment is not without drawbacks, and an examination of the sources of error and limits of results have not been presented in detail. This manuscript addresses some of these issues using examples of poly(*n*-hexyl isocyante) (PHIC), which is a moderately stiff, helical polymer that has been studied extensively in several solvents, and a less stiff polymer, poly[2,7-(9,9 di-*n*-hexylfluorene)] (PHF).

2. Experimental

2.1. Materials

Poly(*n*-hexyl isocyanate) Cat. No. 19249 was purchased from Polysciences, Inc. The material was purified by dropwise addition with stirring of 40 mL methanol to 0.45 g of PHIC dissolved in 50 mL dichloromethane. The precipitate was isolated by filtration, and the process was repeated two additional times. The final product (50% yield) was dried under vacuum at room temperature for 24 h. The predominant impurities were low-molar-mass oligomers and a cyclic trimer identified by MALD/I-TOF MS, which are presumed to be thermal decomposition products [1]. The weight-average molar mass measured by light scattering was 108,000 and $\bar{M}_w/\bar{M}_n = 2.1$. The purified sample was stored at 5 °C.

Monomer 9,9′-dihexyl-2,7-dibromofluorene was synthesized from 2,7-dibromofluorene (Sigma-Aldrich Chemical) and *n*-hexylbromide under basic conditions [2]. Monomer 9,9-dihexylfluroene-2,7-bis(2-dimethyltrimethyleneborate) was synthesized from 9,9′-dihexyl-2,7-dibromofluorene in two steps [3]. Poly[2,7-(9,9 di-*n*-hexylfluorene)] was synthesized by Suzuki coupling. Equal moles of 9,9′-dihexyl-2,7-dibromofluorene (4.15 g, 8.4 mmol) and 9,9-dihexylfluroene-2,7-bis(2-dimethyltrimethyleneborate) (4.71 g, 8.4 mmol) were dissolved in 38 mL of toluene. To this solution was added 2 M Na_2CO_3 aqueous solution (3 equiv to monomer, 12.6 mL) and phase transfer catalyst Aliquat® 336 (0.13 equiv to monomer). The reaction mixture was bubbled with dry nitrogen for 15 min and catalyst tetrakis(triphenylphosphine)palladium (0.03 equiv to monomer, 0.29 g) was added. The reaction was heated under vigorous reflux for 24 h. A small amount of phenylboronic acid was added to end-cap bromo endgroups, and the reflux continued for 4 h. Then a small amount of bromobenzene was added for end-capping of boronate endgroups followed by an additional 4 h reflux. The reaction was poured into 200 mL of methanol. The precipitated polymer was washed with methanol, dilute HCl solution, and dried. The polymer was dissolved in 250 mL of toluene and extracted with 25 g of sodium diethyldithiocarbamate in 200 g of water at 65 °C overnight. The extraction was repeated once. The toluene layer was washed with water and concentrated. The polymer was precipitated in methanol twice and extracted with acetone using a Sohxlet setup overnight to remove low-molecular-weight species. The polymer was dried under vacuum to give 4.75 g (85% yield) of a light yellow solid. The weight-average molar mass of the PHF measured by light scattering was 15,600 with $\bar{M}_w/\bar{M}_n = 1.8$.

2.2. Instrumentation

Uninhibited HPLC-grade THF was used as the SEC eluent with three Polymer Laboratories Plgel mixed-C columns. Instrumentation consisted of a Waters Corporation 2695 solvent delivery and sample management module, a Waters 2487 dual wavelength spectrophotometric (UV) detector, a Precision Detectors PD 2020 two-angle light scattering detector, a Waters 410 differential refractive index (DRI) detector, and a Viscotek H502A differential viscometer. The spectrophotometric and light scattering detectors were connected in serial order after the columns, and the viscometer was connected with a parallel split to the DRI detector after the light scattering detector. Flowrates were nominally 1.0 mL/min or lower. Samples contained 0.2% acetone as a flow marker, and all injection volumes were 100 μL. A universal calibration curve was constructed from 15 narrow-distribution Polymer Laboratories polystyrene standards between molar masses of 580 and 1,300,000.

The two-angle light scattering data analysis assumes a particle shape to calculate root-mean-square radii [4]. For sizes smaller than $R_g \sim 80$ nm, the results for a rod and random coil differ by less than 2% [5,6]. For this work we chose the random coil model. The molar mass range of PHIC overlaps the range examined by Murakami et al. [7], and following their findings that depolarization of scattered light was insignificant for PHIC, no depolarization correction was made.

The specific refractive index increment of PHIC in THF was 0.092 mL/g at 680 nm, measured from the integrated

DRI detector response referenced to dn/dc = 0.184 mL/g for polystyrene. Recent results have confirmed that estimation of dn/dc from the DRI response, obtained at a different wavelength (930 nm) than the light scattering photometer, provides acceptable approximations [8]. The dn/dc of poly[2,7-(9,9 di-*n*-hexylfluoreneone)] was determined to be 0.243 mL/g.

PHIC strongly absorbs UV radiation, and the UV chromatogram at 270 nm provides signal-to-noise and baseline stability that are superior to the DRI response. Normalized chromatograms of the DRI and UV responses superimposed perfectly, so we used the integrated DRI chromatogram to estimate dn/dc, but the more sensitive UV chromatogram for the calculation of local molar masses and viscosities at each retention volume.

No smoothing was applied to any detector signals. Each sample was injected twice and the data files of the two injections were averaged. The light scattering and viscometry detectors were calibrated, and interdetector volumes were determined by a systematic approach that involves superposition of the log M and log[η] calibration curves of a broad polystyrene sample obtained from the respective molar-mass-sensitive detectors on the polystyrene narrow standard calibration curves [9]. A minor axial dispersion correction [10] was made to the local light scattering molar masses and local intrinsic viscosities with a variance of the single species chromatogram $\sigma = 0.15$ mL.

A limited number of experiments were conducted on PHIC in a Waters GPC2000 at 30 °C with dichloromethane as the eluent. The instrument was equipped with a Precision Detectors PD2040 light scattering detector and DRI concentration detection (no viscometry or UV detection). Injection volumes were 0.22 mL, and the flowrate was nominally 0.7 mL/min. The specific refractive index of PHIC in dichloromethane was 0.072 mL/g.

3. Results and discussion

SEC/light scattering detection measures the *Z*-average root-mean-square radius and weight-average molar mass at each retention volume of the SEC chromatogram. The averages are referred to as local quantities, i.e. the value of radius and mass at each retention volume. We will assume that the polydispersity of the local quantities is small and, for the remainder of the manuscript, denote the radii and molar mass quantities at each retention volume as monodisperse quantities R_g and M, respectively. Additional qualifications of these quantities are important. Local averages are often calculated with the assumption that virial terms are negligible at the low concentrations used in SEC. If this assumption does not hold, the local molar mass is an apparent value. Also, the interdetector volume between the light scattering and concentration detector must be taken into account for the calculation of M, but it is not needed in the calculation of R_g, which uses only the light scattering detector signals. Therefore, an incorrect interdetector volume creates an error in M, but not in R_g. We begin with this awareness that the local molar mass might be an apparent value, but assume that the interdetector volume is correct. The two local quantities M and R_g are then related according to the familiar KP model without excluded volume,

$$R_g^2 = \frac{l_p M}{3M_L} - l_p^2 + \frac{2l_p^3 M_L}{M} - \frac{2l_p^4 M_L^2}{M^2}\left(1 - e^{-\frac{M}{l_p M_L}}\right) \quad (1)$$

The two adjustable parameters are l_p and the molar mass per unit contour length, M_L.

Data for PHIC in THF and dichloromethane are presented in Fig. 1. Conformation plots of R_g and M characteristically exhibit scatter in the data at very high and very low molar masses for which either the concentration or light scattering signals are weak. The noisiest data are excluded from Fig. 1 in order to include those points for which the variances in R_g are approximately constant. The two adjustable parameters l_p and M_L were obtained by a least-squares non-linear regression fit of the data to Eq. (1), recognizing that the condition of zero error in the x-values for least-squares minimization is not strictly met. Values obtained for PHIC in THF were $l_p = 40 \pm 2$ nm, $M_L = 730 \pm 15$ nm^{-1} and in dichloromethane $l_p = 23 \pm 2$ nm, $M_L = 730 \pm 30$ nm^{-1}. A few literature values are available for PHIC in THF. Berger and Tidswell [11] reported $l_p =$ 42.5 nm, which agrees reasonably with our results, although their assumed value of $M_L = 635$ nm^{-1} is considered low. Estimates of l_p from the limited data set of Yu [12] in THF are high because the *Z*-average root-mean-square radius of polydisperse fractions was used [13]. A curve presented recently by Cotts [14] does not report l_p estimates but appears to have higher R_g, values at similar molar masses than our results. There are several values reported in *n*-hexanes. The values measured by Murakami et al. [7] of

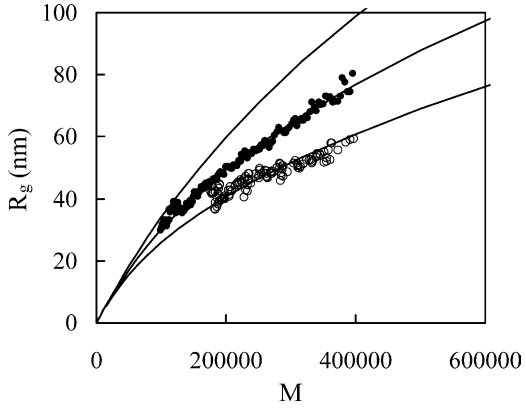

Fig. 1. Root-mean-square radii conformation plots for PHIC in THF (solid symbols) with total mass injected = 0.1864 mg and flowrate = 1.0 mL/min, and dichloromethane (open symbols) with total mass injected = 0.2708 mg and flowrate = 0.7 mL/min. The solid lines from top to bottom are predictions from Eq. (1) using $M_L = 730$ nm^{-1} and $l_p = 80$, 40, and 23 nm, respectively.

$l_p = 42 \pm 1$ nm and $M_L = 715 \pm 15$ were from an extensive range and number of narrow molar mass distribution samples, and are similar to other results in hexane [15,16] and toluene [11,17]. The general consenus is $l_p = 40$–43 nm and $M_L = 700$–$740\ \text{nm}^{-1}$ for PHIC in non-halogenated solvents. Our values for PHIC in THF are in reasonable agreement. Persistence lengths measured in chlorinated solvents dichloromethane [17] ($l_p = 21$ nm and $M_L = 750\ \text{nm}^{-1}$) and *n*-butyl chloride [18] ($l_p = 35$ nm and $M_L = 760\ \text{nm}^{-1}$) are lower, reportedly because of local interactions between the halogenated solvents and PHIC amide groups [19], resulting in greater local flexibility. Our results agree with the previously reported values for dichloromethane.

PHIC has a low specific refractive index increment in THF and one that is even lower in dichloromethane. Even at the fairly high sample injection concentrations used to obtain the data in Fig. 1, there is considerable noise in the high and low mass regions, and the molar mass range spans less than a decade. In fact, Fig. 1 is plotted with linear *y*- and *x*-axis scales to more clearly depict the data set because of its narrow range. Conformation plots usually cover a broader mass range and are presented with log–log scales. Similar results were obtained at injection concentrations down to 0.5 mg/mL but with more scatter in the data because of weaker light scattering signals. The accuracy of the results at several concentrations is somewhat surprising considering the obvious concentration dependence on the shapes of the UV concentration chromatograms (Fig. 2). We shall return to this point later when viscometry detection results are discussed.

A popular method for obtaining the two adjustable parameters l_p and M_L, given by Murakami et al. [7], is an approximation for Eq. (1),

$$\left(\frac{M}{\langle R_g^2\rangle}\right)^{1/2} = \left(\frac{3M_L}{l_p}\right)^{1/2}\left[1 + \frac{3l_pM_L}{2M}\right] \tag{2}$$

for cases where $M/(2l_pM_L) > 2$, with error of less than 1%.

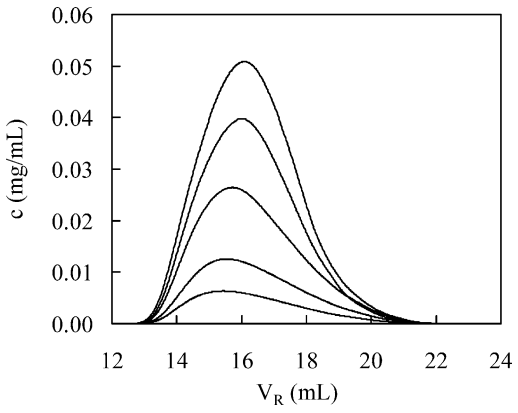

Fig. 2. UV (270 nm) chromatograms of PHIC at a flowrate of 1.0 mL/min, sample injected at concentrations of 1.8639, 1.4521, 1.0202, 0.4950, and 0.2475 mg/mL.

The parameters l_p and M_L are evaluated from the intercept $(3M_L/l_p)^{1/2}$ and slope $3M_L(3l_pM_L)^{1/2}/2$ of $(M/\langle R_g^2\rangle)^{1/2}$ plotted versus M^{-1}. Data are plotted for PHIC in THF and dichloromethane in Fig. 3. Reasonable estimates of $l_p = 40$ nm and $M_L = 730\ \text{nm}^{-1}$ are obtained from the data in THF, but the data for dichloromethane data are unsuitable for least-squares linear regression. There is a well-known problem of possible spurious correlations in plots with the same variable (in this case, molar mass) plotted in both the ordinate and abscissa, which is worsened with the use of ratios of the variables with potentially unpredictable variances in the *y*-axis values (e.g. see Ref. [20]). Both are operative, particularly with SEC data that span a limited molecular size and molar mass range. The situation is worsened with the data intervals of the *x*-axis values. SEC data are obtained at approximately equally spaced log *M* intervals. The *x*-values are no longer equally spaced on the reciprocal *M* plot, which can make a few data points at low molar mass—where noise becomes problematic—influential data points for least-squares regression. These statistical difficulties do not always invalidate the use of plots, based on Eq. (2) to illustrate a relationship, as shown for the data in THF. The data for dichloromethane suggest that the method should be applied with extreme caution, and that directly solving Eq. (1) is a preferred approach. We note, parenthetically, that a recent evaluation [21] of extrapolation methods to determine unperturbed dimensions from SEC/light scattering detection contains several examples of noisy plots with ratios of *M* and/or R_g plotted in both the *x*- and *y*-axes.

The example of measuring l_p for PHIC from *M* and R_g data obtained from SEC/light scattering suggests that reasonable estimates of l_p can be obtained on a single broad molar mass distribution sample. This PHIC sample contains molecules with sizes that can be measured by light scattering detectors with incident sources of 680 nm, and the polymer is sufficiently stiff to not exhibit excluded volume effects, which would manifest themselves as upward

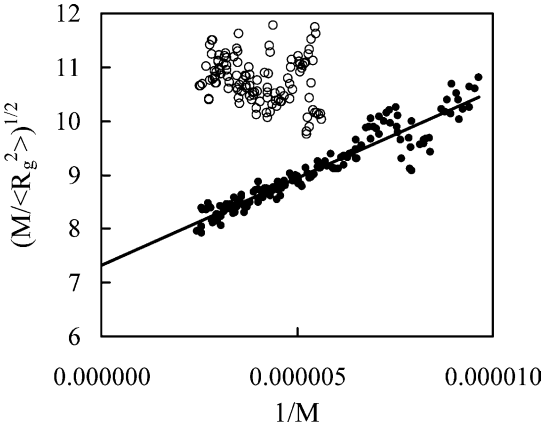

Fig. 3. Plot according to Eq. (2) for PHIC in THF (solid symbols) and dichloromethane (open symbols), same conditions as in Fig. 1. Solid line is an unweighted least-squares regression linear fit.

curvature in the high mass region of the R_g–M conformation plots. The molar mass distribution of this PHIC sample covers the range of Kuhn statistical elements $N=L/b$ of 0.33–13.7, with $L/b=1.8$ at the weight-average molar mass. The largest size in the PHIC distribution is well below the critical value $L/b\sim50$ for the onset of excluded volume effects [22], and the largest measurable size is limited to the exclusion limit for the SEC column set, which is $R_g\sim80$. Unfortunately, we are limited by the wavelength of incident light to examining macromolecules with sizes greater than $R_g\sim10$ nm, which limits the accessible R_g and M ranges to less than a decade.

In comparison, differential viscometry responses are exceptionally strong for this and all rigid polymers, and they can be measured at very low molar masses, making viscosity-molar mass conformation plots a desirable alternative to R_g–M plots. The differential viscometer measures the specific viscosity at each retention volume, η_{sp}, which can be combined with the concentration detector response at each retention volume to provide local values η_{sp}/c. At the low concentrations of SEC, this local value approximates the zero concentration quantity, or local intrinsic viscosity $[\eta]$, which can also be used to calculate a local molar mass from a universal calibration curve. This local molar mass from the universal calibration curve is a number-average, and analogous to light scattering local quantities, it is implicitly assumed that the polydispersity of the local value is negligible, and the local value is again M. The estimation of stiffness parameters from hydrodynamic data has been the subject of considerable interest and study and has been summarized in texts on solution properties of rigid polymers [23,24]. A common starting point is the cylindrical wormlike chain model for intrinsic viscosity, without excluded volume effects, of Yamakawa, Fujii, and Yoshizaki [25,26] (from here on referred to as the Y–F–Y model) that predicts the viscosity of a bending spherocylinder in the rod-like region for molecules with contour length, L, up to dimensions $L/b\leq2.278$ (b is the Kuhn statistical length),

$$[\eta]=\frac{2\pi N_A M^2 f(L/b)}{45M_L^3F_\eta(p)} \tag{3}$$

where $p=L/d$, d is the wormlike chain hydrodynamic diameter, and $f(L/b)$ and $F_\eta(p)$ are functions of L/b whose coefficients are provided in Yamakawa's papers. At values of $L/b\geq2.278$,

$$[\eta]=\frac{M}{\Phi_\infty^{-1}\left(\frac{M_L}{b}\right)^{3/2}M^{1/2}\varphi(L,d,b)} \tag{4}$$

where $\Phi_\infty=2.87\times10^{23}$, and $\varphi(L,d,b)$ is a function of b/L and d/b.

Similar to Eq. (2), a popular approach to estimating wormlike chain parameters from the Y–F–Y model is through linear approximations. Bushin [27] and Bohdanecký [28] showed that the Y–F–Y model could be approximated by

$$\left(\frac{M^2}{[\eta]}\right)^{1/3}=A_\eta+B_\eta M^{1/2} \tag{5}$$

where the intercept is

$$A_\eta=\frac{A_0M_L}{\Phi_\infty^{1/3}} \tag{6}$$

$$A_0=0.46-0.53\log d_r \tag{7}$$

and the slope is

$$B_\eta=\frac{B_0}{\Phi_\infty^{1/3}}\left(\frac{2l_p}{M_L}\right)^{-1/2} \tag{8}$$

for

$$B_0=1.00-0.0367\log d_r \tag{9}$$

with $d_r=d/2l_p$. B_0 is a slowly decreasing function of d_r and, to a first approximation, is replaced by its mean value, 1.05. The approximation holds over a range of $M/(2l_pM_L)$ from 0.4 to 300, making this a practically useful method for estimating l_p from viscometric data. However, the three parameters l_p, M_L, and d cannot be obtained independently without additional information or by approximations discussed in Bohdanecký's paper. The R_g and M data from SEC/light scattering results for PHIC and reported literature values indicate that $M_L\sim730\,\text{nm}^{-1}$ and $l_p\sim40$ nm, allowing us to examine the results of Eq. (5) by fixing either quantity and evaluating the other two from the slope and intercept. The data for PHIC at an injection concentration of 1.8639 mg/mL, using M values from light scattering detection and η_{sp}/c from viscometry detection, are shown in Fig. 4. The plot, again, uses ratios in the y values and plots M in both the y- and x-axes, but appears linear and considerably less noisy than the analogous linear approximation for root-mean-square radii (Eq. (2) and Fig. 3), mainly because it covers a larger mass range, and the local viscosities have smaller variances than local R_g

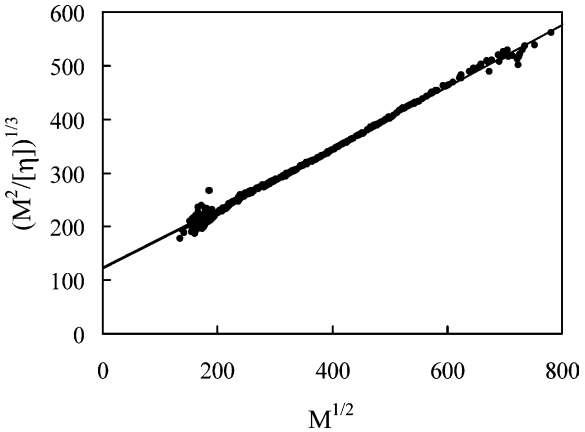

Fig. 4. Bohdanecký plot for PHIC, injection concentration 1.8639 mg/mL, flowrate 1.0 mL/min.

values. The apparent improvement in the data is deceptive. With M_L set to 730 nm^{-1}, we obtain $l_p = 29$ nm, which is considerably lower than values reported in the literature for PHIC in THF. Also, the best value for the tube diameter, $d = 3$ nm, that fits the data with the Y–F–Y model (Fig. 5) is unreasonably large compared to reported values between 1.5 and 2 nm. We are, in fact, unable to find any reasonable set of l_p, M_L, and d parameters by any fitting procedures for the Y–F–Y model. Cognizant of the concentration dependence on the shapes of chromatograms shown in Fig. 2, the results for a lower sample injection concentration (Fig. 6) are possibly closer to the expected result, but the lower sample concentration results in weak light scattering signals and accompanying noise and a reduced molar mass range in the conformation plot. The problem lies in the fact that the local viscosity and molar mass quantities are sensitive to concentration, shown in Figs. 7 and 8. The local M and η_{sp}/c values are apparent values that are extrapolated to zero concentration at fixed retention volumes in Figs. 9 and 10. These figures should not be confused with the familiar Huggins plots of specific viscosity and light scattering plots that extrapolate to zero concentration in order to account for intermolecular interactions (virial terms). Rather, Figs. 9 and 10 are extrapolating the local M and η_{sp}/c quantities that are changing with concentration because of changes in chromatogram shapes, i.e. large molecules are eluted later with increasing concentration. The extrapolated values are fitted with reasonable values for the Y–F–Y model in Fig. 11.

Sample concentration effects in the SEC of semiflexible polymers have not been discussed in detail but apparently have been recognized and avoided in the SEC of PHIC by Gu et al. [40] in chloroform and Cotts [14] in THF. The former ran SEC samples at 0.01 mg/mL, the latter at 0.44 mg/mL. Our experiments in THF were repeated at flowrates between 1.0 and 0.3 mL/min on the 5 μm particle-diameter packing material and also on Toso Haas 13 μm particle-diameter packing material. We estimate the shear rates in the columns [29] range from a maximum of 4470 s^{-1} for the 5 μm columns operating at 1.0 mL/min to a low of 516 s^{-1} for the 13 μm particle columns at 0.3 mL/min. The shear rates in the differential viscometer are estimated assuming a 50:50 split of the flow in the differential bridge as 5180 and 1550 s^{-1} for 1.0 and 0.3 mL/min, respectively. We observed very subtle differences in the high-molar-mass regions of chromatograms, where the differential viscometer response increases slightly with decreasing flowrate. There is only a minor effect on the local viscosities and no noticeable effects on local molecular weights from light scattering. The results suggest minor non-Newtonian behavior in the high-molar-mass regions of the distributions and no detectable shear degradation of PHIC. We conclude that most of the problems with the estimation of parameters by the Y–F–Y method and the linear approximations described by Eqs. (5)–(9) for the moderately stiff PHIC are attributed to concentration effects that cause chromatogram peak shape changes rather than shear degradation,

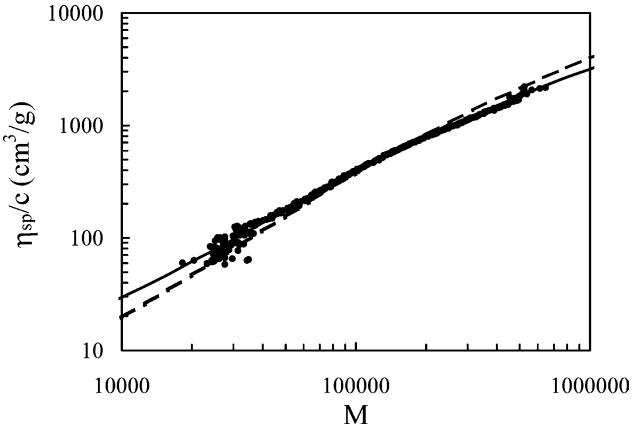

Fig. 5. Viscosity conformation plot for PHIC, 1.8639 mg/mL injection concentration. Solid line is best fit of Y–F–Y model to data for $l_p = 26$ nm, $M_L = 730$ nm^{-1}, $d = 3$ nm. Dashed line is Y–F–Y fit with $l_p = 40$ nm, $M_L = 730$ nm^{-1}, $d = 1.8$ nm.

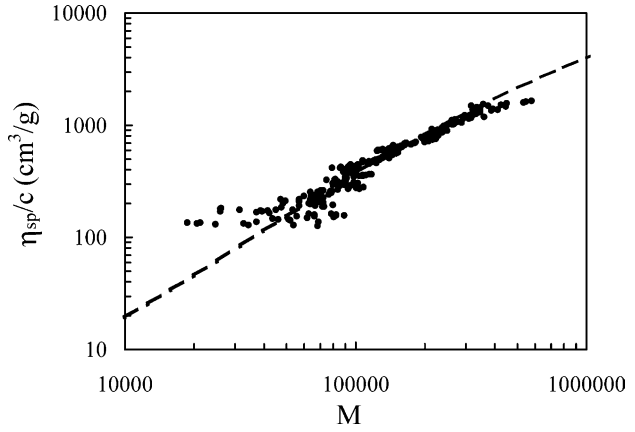

Fig. 6. Viscosity conformation plot for PHIC, 0.2475 mg/mL injection concentration. Dashed line is Y–F–Y fit with $l_p = 40$ nm, $M_L = 730$ nm^{-1}, $d = 1.8$ nm.

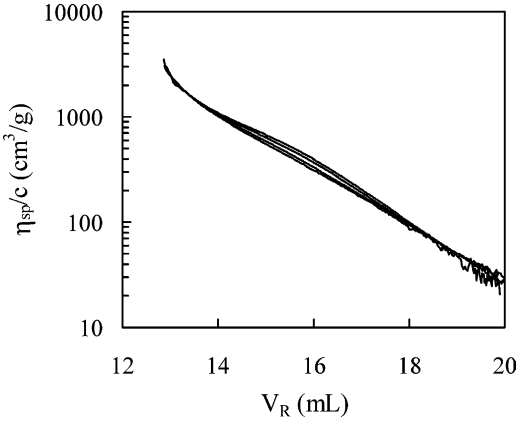

Fig. 7. Local viscosity calibration curves for PHIC at, from top curve to bottom, injection concentrations of 1.8639, 1.4521, 1.0202, 0.4950, and 0.2475 mg/mL.

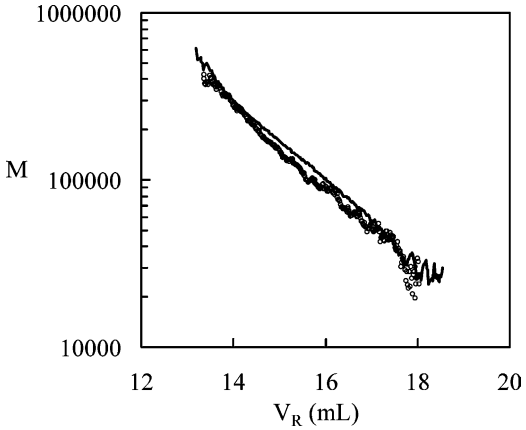

Fig. 8. Local molar mass calibration curves from light scattering detection for PHIC at 1.8639 mg/mL (solid line, upper curve) and 1.0202 mg/mL (symbols, lower curve). For clarity, only two concentrations are shown.

non-Newtonian response of the viscometry detector, or failure in the Y–F–Y model and related approximations.

A polymer less rigid and of lower molar mass than the above PHIC sample provides an example for which the SEC-viscometry experiment is optimal and the methods for estimating wormlike chain parameters work quite well. M from light scattering detection and $[\eta]$ from the viscometry detector are plotted in Fig. 12 for poly[2,7-(9,9 di-*n*-hexylfluorene)]. The linear approximation method (Fig. 13) and non-linear regression of the Y–F–Y model provide equivalent results and give $l_p = 8.0$ nm and $d = 0.90$ nm, assuming $M_L = 410\ \text{nm}^{-1}$. The estimates are close to literature values for similar polymers: $l_p = 8.5$ nm for poly[2,7-(9,9 di-*n*-octylfluorene)] in THF [30], 7 nm for poly{2,7[-(9,9 bis 2-ethylhexyl) fluorene]} in toluene [31], and 9.5 nm for poly{2,7-[9,9-bis((*S*)-3,7-dimethyloctyl)]-fluorene} in THF [32]. The authors of [32] used the touched-bead Kratky–Porod model of Yoshizaki [33] to estimate persistence length, and we have included the touched-bead prediction for $l_p = 8.0$ nm $d = 0.74 d_b = 0.90$ nm (d_b is the bead diameter) and $M_L = 415\ \text{nm}^{-1}$ in Fig. 12. The touched-bead model predicts slightly higher viscosity at low molar

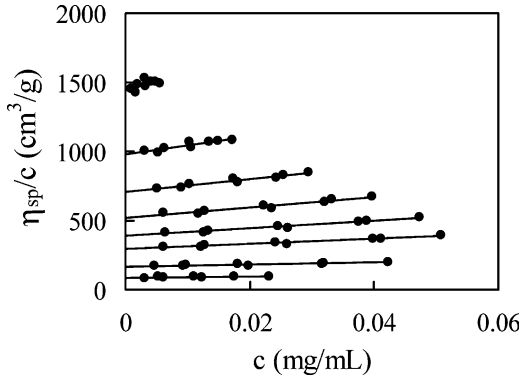

Fig. 9. Viscosity extrapolations to zero concentrations at fixed retention volumes. From top to bottom, $V_r = 13.5$, 14, 14.5, 15, 15.5, 16, 17, and 18 mL.

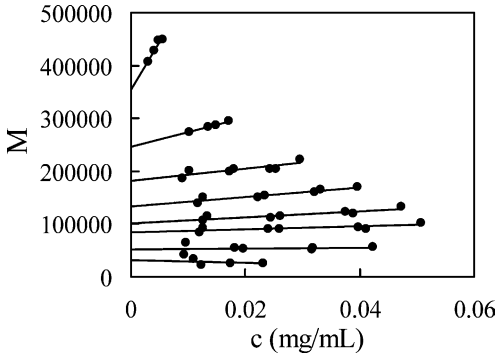

Fig. 10. Light scattering detection molar mass extrapolations to zero concentration at fixed retention volumes given in Fig. 9.

masses. Fitting our data with the touched-bead model results in $l_p \sim 9$ nm and an equivalent cylindrical model tube diameter of 0.7 nm; both values seem somewhat unreasonable for PHF. We have not evaluated more complicated five-parameter helical wormlike chain models. Chromatograms exhibit no significant concentration effects for sample concentrations less than 4 mg/mL. The molar mass distribution of this sample covers the range $L/b = 0.2$–11.9, with $L/b = 2.3$ at the weight-average molar mass. These values are similar to the PHIC sample, and they are also below the critical $L/b \sim 50$ for onset of excluded volume effects.

The results for PHF suggest that SEC-viscometry data are suitable for estimating wormlike chain parameters of polymers of low molar mass with low to moderate rigidity. We caution, however, that M from light scattering and $[\eta]$ from viscometry require two interdetector volumes—one between the differential viscometer and the concentration detector, and another between the light scattering and concentration detectors. An incorrect interdetector volume can rotate and distort conformation plots, with effects described by some as 'spectacular and insidious' [34]. Minimizing the product of the slope of the molar mass calibration curve and σ, as described by Jackson and Yau

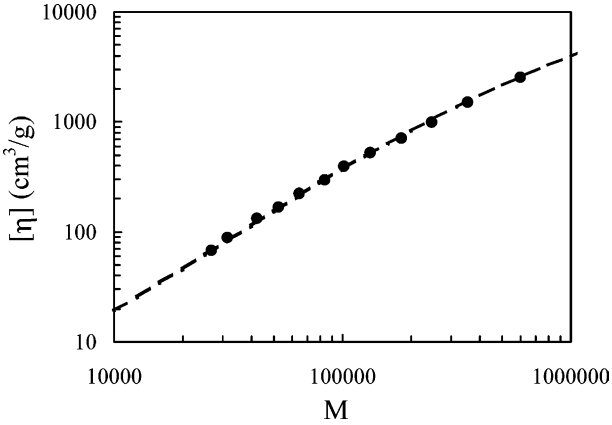

Fig. 11. Viscosity conformation plot for PHIC using viscosity and molar mass data extrapolated to zero concentration (solid symbols). Dashed line is Y–F–Y fit with $l_p = 40$ nm, $M_L = 730\ \text{nm}^{-1}$, $d = 1.8$ nm.

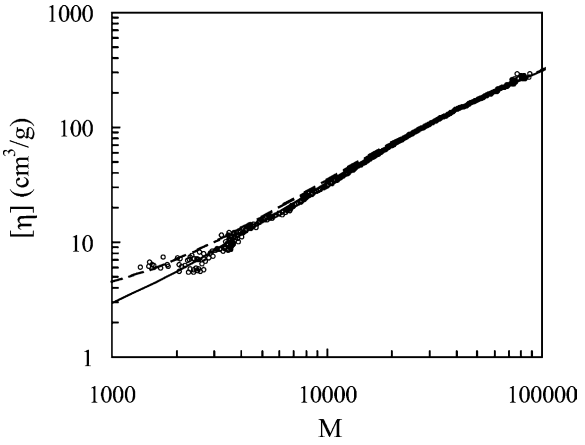

Fig. 12. PHF with Y–F–Y model predictions for $M_L = 415\ \mathrm{nm}^{-1}$ and $d = 0.9$ nm for $l_p = 8$ nm (solid line), and touched-bead model prediction (dashed line) for the same values of M_L and l_p, with $d_b = 0.74d$.

[35], eliminates much of the problem, which we have attempted to do in this study. The errors also become less significant in samples with broad molecular size distributions. We also note that local quantities M and $[\eta]$ are correlated through c measured by the concentration detector, and error in the latter can seriously affect the results from any of the data treatment methods.

The local molecular weight can also be calculated from the local intrinsic viscosity and a universal calibration curve, although the validity of this method has been questioned for rigid chains that drain freely [36], which recently led Dondos to estimate Flory's universal constant for various rigid polymers that present a draining effect [37]. Some disagreement still exists because others have reported the validity of universal calibration for rodlike homopolypeptides in DMF [38,39] and for PHIC in chloroform [40]. The results for poly[2,7-(9,9 di-*n*-hexylfluorene)] are not much different than those obtained from local molar masses from light scattering (Fig. 14) suggesting that for moderately stiff polymers, such as PHF, either M from SEC/light scattering or M from SEC/viscometry and

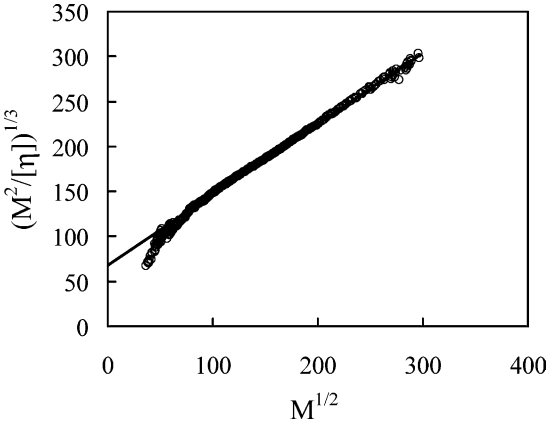

Fig. 13. Bohdanecký plot for PHF, injection concentration 3.065 mg/mL, flowrate 1.0 mL/min.

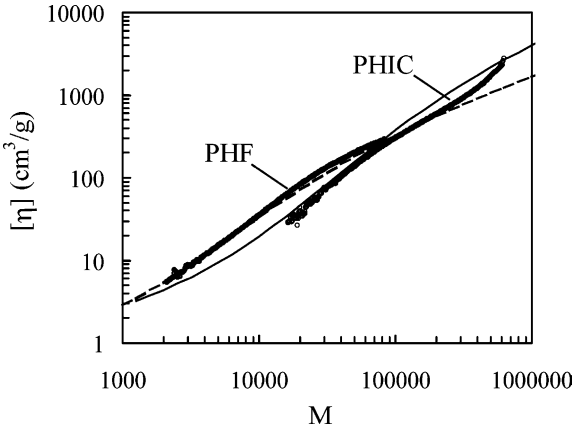

Fig. 14. PHIC (injected concentration = 0.2475 mg/mL) and PHF conformation plots for local molar masses calculated from viscometry detection and the universal calibration curve. Solid and dashed lines are Y–F–Y best fits for PHIC and PHF, respectively.

universal calibration can be used. PHF is as stiff as some polyamides and cellulosics, not as stiff as PHIC and other rigid polymers ($l_p \sim 40$ nm), but more rigid than flexible polymers ($l_p \sim 1$ nm). The results for PHIC, at the lowest concentration investigated, are erroneous at high molar masses. This might suggest that the freely draining properties of this polymer are significant and the non-draining assumption inherent in calculating local molar masses from the universal calibration curve is inappropriate for moderate to highly rigid polymers. However, given the severe concentration dependence on chromatogram peak shapes, we cannot ignore the possibility of an experimental or artifactual explanation for this apparent failure of universal calibration.

An alternative to the application of the Y–F–Y model proposed by Dondos [41,42] uses limited regions of the molar mass—intrinsic viscosity conformation plot to estimate persistence lengths. At high molar masses, the statistical segment length is obtained from the unperturbed dimensions parameter by the method of Stockmayer–Fixman [43] and Burchard [44]. The scaling exponents in the high mass region for our data are ~1.1 for PHIC and 0.9 for PHF, indicating that the plateau region has not been reached, and this method is inappropriate for our PHIC and PHF data. At molar masses similar to or smaller than a statistical length, the DB method cannot be used. This leaves only the transition region between rod and random coil, for which the authors propose plotting $1/[\eta]$ against $M^{1/2}$,

$$\frac{1}{[\eta]} = -A_2 + \frac{1}{K_\theta M^{1/2}} \tag{10}$$

from which the slope $1/K_\theta$ is used to estimate the persistence length:

$$2l_p = \left(\frac{K_\theta}{\Phi}\right)^{2/3} M_L \tag{11}$$

The draining parameter Φ is an empirical function of the Mark–Houwink exponent a, given in Dondos' paper. Plots, according to Eq. (10) of SEC data for PHIC and PHF, are shown in Fig. 15. Only the very highest molar mass points apply, as shown by the tangents on the plot. These regions give persistence length estimates of $l_p = 32$ nm with $M_L = 730\ \text{nm}^{-1}$ for PHIC, and $l_p = 7$ nm with $M_L = 405\ \text{nm}^{-1}$ for PHF. Both values are low compared to the estimates obtained from the Y–F–Y model. We cannot evaluate if the estimates are low because of the uncertainty in obtaining the tangential slopes or from a limitation in the proposed method (see Ref. [45] for further discussion). This method uses only a small fraction of the available data, and as such, does not seem to be a good choice for determining wormlike chain parameters from multidetector SEC data on a single sample.

Finally, we refer to the determination of the monomeric unit projection length from SEC and viscometry proposed by Gonzalez et al. [46]. This method relies on a universal calibration curve and the assumption that the Flory Universal draining factor is constant. This is not expected to hold for freely and partially draining rigid polymer chains, and in our opinion, it prevents the application of this method to SEC data of stiff and semiflexible polymers.

4. Conclusions

Wormlike chain parameters can be estimated from SEC/light scattering data, even in the presence of severe concentration effects that change chromatogram peak shapes. However, the size range is limited by the wavelength of incident light, and polymers with low dn/dc, such as PHIC, can be problematic. Methods that approximate the root-mean-square radius—molar mass relationship of the Kratky–Porod model, in linear form, are sensitive to noise and are not preferred for SEC data. Viscometry detection covers a broader molar mass range and natively has stronger signals than light scattering detection, but stiff polymers, such as PHIC, exhibit severe concentration dependences that make the data analysis methods unsuitable unless the local viscosities and apparent molar masses are extrapolated to zero concentration values. Use of the universal calibration curve to calculate local molar masses from local intrinsic viscosities is not suitable for these polymers. Finally, methods that use only the data in the rodlike-to-Gaussian coil transition region are of limited and possibly dubious utility. A sensible strategy for measuring persistence lengths of very stiff, high molar mass polymers is to use light scattering detection and the K–P wormlike chain model; and for low molar mass polymers of moderate stiffness, to apply the Y–F–Y hydrodynamic cylindrical model to viscometry detection data. Both methods must be confined to data with an upper bound in molar mass defined by $L/b < 50$ to avoid excluded volume effects.

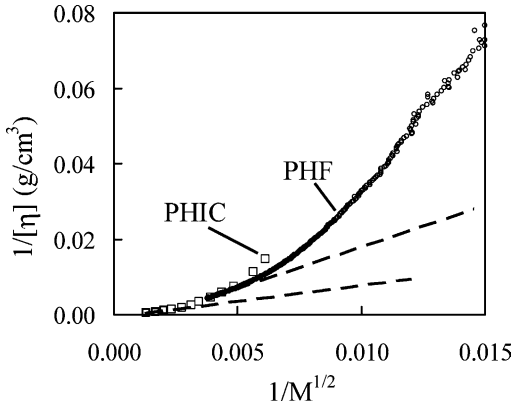

Fig. 15. Plots based on Eq. (10) for PHIC and PHF. Dashed lines are tangent slopes used to estimate l_p with Eq. (11) and the method of Dondos [41,42].

Acknowledgements

The authors thank Andrew Hoteling for obtaining MALDI spectra. TM thanks Hyuk Yu, Steve Balke, Dennis Massa, Jehuda Greener, Jim Elman, and Charles Lusignan for helpful discussions and suggestions.

References

[1] Durairaj B, Dimock AW, Samulski ET, Shaw MT. J Polym Sci, Part A: Polym Chem 1989;27:3211.
[2] Woo EP, Shiang WR, Inbasekaran M, Roof GR. US Patent 5,708,130; 1998.
[3] Zheng S, Shi J. Chem Mater 2001;13(12):4405.
[4] Mourey TH, Coll H. Hyphenated techniques in polymer characterization. In: Provder T, editor. ACS advances in chemistry series, vol. 247. Washington, DC: American Chemical Society; 1995. p. 123–40.
[5] Mourey TH, Coll H. J Appl Polym Sci 1995;56:65.
[6] Frank R, Frank L, Ford N. Hyphenated techniques in polymer characterization. In: Provder T, editor. ACS advances in chemistry series, vol. 247. Washington, DC: American Chemical Society; 1995. p. 109–22.
[7] Murakami H, Norisuye T, Fujita H. Macromolecules 1980;13:345.
[8] Podzimek S. Multiple detection in size-exclusion chromatography. In: Striegel AM, editor. ACS symposium series, vol. 893. Washington, DC: American Chemical Society; 2005. p. 94–112.
[9] Mourey TH, Balke ST. Chromatography of polymers. Characterization by SEC and FFF. In: Provder T, editor. ACS symposium series, vol. 521. Washington, DC: American Chemical Society; 1993. p. 199–219.
[10] Hamielec AE. J Liq Chromatogr 1980;3:381.
[11] Berger MN, Tidswell BM. J Polym Sci Polym Symp 1973;42:1063.
[12] Fetters LJ, Yu H. Macromolecules 1971;4:385.
[13] Yu H. Private communication.
[14] Cotts PM. Multiple detection in size-exclusion chromatography. In: Striegel AM, editor. ACS symposium series, vol. 893. Washington, DC: American Chemical Society; 2005. p. 52–75.
[15] Rubingh DN, Yu H. Macromolecules 1976;4:681.
[16] Jinbo Y, Teranuma O, Kanao M, Sato T. Macromolecules 2003;36: 198.
[17] Itou T, Chikiri H, Teramato A, Aharoni SM. Polym J 1988;20:143.

[18] Kuwata M, Murakami H, Norisuye T, Fujita H. Macromolecules 1984;17:2731.
[19] Cook R, Johnson RD, Wade CG, O'Leary DJ, Muñoz B, Green MM. Macromolecules 1990;23:3454.
[20] Berges JA. Limol Oceanogr 1997;42:1006.
[21] Búrdalo J, Medrano R, Saiz E, Tarazona MP. Polymer 2000;41:1615.
[22] Norisuye T, Fujita H. Polym J 1982;14:143.
[23] Yamakawa H. Helical wormlike chains in polymer solutions. New York: Springer; 1997.
[24] Tsvetkov VN. Rigid-chain polymers. New York: Consultants Bureau; 1989.
[25] Yamakawa H, Fujii M. Macromolecules 1974;7:128.
[26] Yamakawa H, Yoshizaki T. Macromolecules 1980;13:633.
[27] Bushin SV, Tsvetkov VN, Lysenko EB, Emel'yanov VN. Vysokomol Soedin 1981;A23:2494.
[28] Bohdanecký M. Macromolecules 1983;16:1483.
[29] Barth HG, Carlin Jr FJ. J Liq Chromatogr 1984;7:1717.
[30] Grell M, Bradley DD, Long X, Chamberlain T, Inbasekaran M, Woo EP, et al. Acta Polym 1998;49:439.
[31] Fytas G, Nothofer HG, Scherf U, Vlassopoulos D, Meier G. Macromolecules 2002;35:481.
[32] Wu L, Sato T, Tang H-Z, Fujiki M. Macromolecules 2004;37:6183.
[33] Yoshizaki T, Nitta I, Yamakawa H. Macromolecules 1988;21:165.
[34] Reed WF. Macromol Chem Phys 1995;196:1539.
[35] Jackson C, Yau WW. J Chromatogr 1993;645:209.
[36] Dubin P, Principi JM. Macromolecules 1989;22:1891.
[37] Dondos A, Papanagopoulos D. J Polym Sci, Part B: Polym Phys 2003; 41:707.
[38] Temyanko E, Russo PS, Ricks H. Macromolecules 2001;34:582.
[39] Dawkins JV, Hemming M. Polymer 1975;16:554.
[40] Gu H, Nakamura Y, Sato T, Teramato A, Green MM, Andreola C. Polymer 1999;40:849.
[41] Dondos A, Staikos G. Colloid Polym Sci 1995;273:626.
[42] Dondos A. Polymer 2000;41:4607.
[43] Stockmayer WH, Fixman M. J Polym Sci 1963;C1:137.
[44] Burchard W. Makromol Chem 1961;50:20.
[45] Horský J, Bohdanecký M. Macromol Theory Simul 1998;7:317.
[46] Gonzalez C, Zamora F, Rodriguez M, Gonzalez M, Leon LM. J Macromol Sci-Phys 1990;B29:337.